

# Deformation-promoted reactivity of single-walled carbon nanotubes

Kausala Mylvaganam and L C Zhang<sup>1</sup>

Centre for Advanced Materials Technology, The University of Sydney, NSW 2006, Australia

E-mail: [kausala@aeromech.usyd.edu.au](mailto:kausala@aeromech.usyd.edu.au) and [zhang@aeromech.usyd.edu.au](mailto:zhang@aeromech.usyd.edu.au)

Received 7 September 2005, in final form 19 October 2005

Published 14 December 2005

Online at [stacks.iop.org/Nano/17/410](http://stacks.iop.org/Nano/17/410)

## Abstract

This paper investigates the effect of mechanical deformation of a single-walled carbon nanotube (SWNT) on its reactivity with hydrogen and alkyl radicals. The influence of individual loading modes was explored with the aid of molecular dynamics simulation for deformation and quantum mechanics analysis for reaction. The study discovered that the radicals bind to the deformation-induced ridges tightly with high binding energies, but at the deformation-flattened surface the binding energy becomes even lower than that of a non-deformed nanotube. At a low strain energy of  $\sim 2 \text{ kJ mol}^{-1}$  a nanotube deformed by central loading gives a stronger binding with a hydrogen atom to the ridge, while at a little higher strain energy pure bending and torsion give rise to a better binding. The above findings show that mechanical deformation of carbon nanotubes can strongly promote their reactivity and form stronger covalent bonds with radicals.

(Some figures in this article are in colour only in the electronic version)

## 1. Introduction

Carbon nanotubes (CNTs) have potential applications in nano-electronic devices such as p–n junctions [1] and gas sensors [2]. These devices are based on the chemical interaction between the CNTs and chemical species that are either in the environment or used in industrial processes. For instance, in the environmental monitoring,  $\text{NO}_2$  that is resulted from combustion and automotive emissions is detected using sensors. Kong *et al* [2] have demonstrated miniaturized chemical sensors based on single-walled CNTs. They found that the electrical resistance of single-walled CNTs increased dramatically with a fast response and high sensitivity upon exposure to  $\text{NO}_2$  gas. Moreover, due to their excellent mechanical properties, CNTs are also considered to be valuable materials for reinforcing polymers, for which a significant load transfer capacity between the nanotube and the polymer is necessary [3]. This requires a strong interfacial interaction between the polymer matrix and the nanotubes. Since covalent bonding at the CNT–polymer interface will make the reinforcement stronger, it is essential to understand deeply the bonding mechanisms and possible improvements of the CNT–polymer reactivity.

<sup>1</sup> Author to whom any correspondence should be addressed.

Bauschlicher [4, 5] and Jaffe [6] have studied the addition of H atoms and F atoms to the free nanotube sidewall using the *ab initio* quantum chemistry approach and got results that are in agreement with experimental data. In our previous works [7, 8] we have demonstrated that covalent bonds between a CNT and polymer chains could be formed either by generating free radicals on the polymer chains or by first functionalizing the nanotube using free radical or anionic initiators followed by adding the monomer units to lead to CNT-grafted polymer. Moreover, we found that the tubes of smaller diameters have higher binding energies [7]. This indicates that the curvature of a CNT may play an important role in the reactivity of radicals with nanotubes. On the other hand, in making CNT-reinforced composites, CNTs must be well dispersed in matrix incorporated with a process of mechanical blending, at which deformation and thus curvature changes of CNTs are significant and unavoidable. This means that the reactivity on the surface of a nanotube may be promoted during mechanical blending.

In this work we will reveal the reactivity of a hydrogen radical and an alkyl radical with a nanotube under some fundamental deformation modes—torsion, centre loading, pure bending, compression, and tension—with the aid of molecular dynamics and quantum mechanics analyses.

## 2. Computational technique

A (17, 0) zigzag nanotube of length  $\sim 75$  Å was subjected to deformation introduced individually by torsion, bending, centre loading, compression, and tension, modelled by the classical molecular dynamics simulation with the Tersoff–Brenner potential [9, 10].

Under the torsional deformation, 10 rows of atoms on each end of the CNT were rotated in opposite directions in steps of  $1^\circ$ . First, these displaced atoms were held rigid at their rotated positions and the rest were relaxed to a minimum energy using the conjugate gradient algorithm. Then the relaxed atoms were held at their new positions and the previously rigid end atoms were relaxed to the minimum energy. This procedure was repeated up to a rotation angle of  $40^\circ$ . Under compressive deformation, two rows of atoms on each end of the CNT were pushed axially in opposite directions at an increment of  $0.1$  Å. These atoms were first held rigid at their positions and the rest were relaxed to a minimum energy using the conjugate gradient algorithm. Then the relaxed atoms were held at their new positions and the previously rigid end atoms were relaxed to the minimum energy. This procedure was repeated until the failure of the CNT. The computational procedures for CNTs under other deformation modes have been described in [11, 12].

The deformed CNTs, before and after buckling, under different deformation modes were selected to compare the reactivity. Those before buckling were selected with the level of strain energy around  $2 \text{ kJ mol}^{-1}$ . To explore this, a small section of the deformed tube was taken and hydrogen atoms were added to the dangling bonds of the perimeter carbons. The geometry of the added hydrogen atoms were optimized while keeping the geometry of the deformed tube section fixed. The reactivity with radicals was examined by placing the radical closer to a ridge or a flattened portion of the nanotube section and its geometry was optimized while keeping the geometry of all the other atoms fixed.

The geometry optimizations were performed using the density functional theory with a hybrid functional B3LYP [13–16] and a 3-21G basis set [17]. For open shell molecular radicals, the unrestricted formalism was used. This level of calculation is known to produce reasonable results for geometries and bond energies [18]. The quantum mechanics calculations were performed on a super-computer using the *ab initio* quantum chemistry package Gaussian 03 [19].

## 3. Results and discussion

On loading, the CNT buckled under all deformation modes except tension. The deformed tubes after buckling are shown in figures 1(a)–(e). All the deformations shown here are within their elastic regions, i.e., on releasing the load they return to their undeformed states. The binding energy of the radicals with nanotubes under various loading conditions, the relative binding energy with respect to the free tube and the C–H bond length are tabulated in tables 1 and 2. Thus a better deformation mode in terms of a stronger chemical bonding can be identified easily.

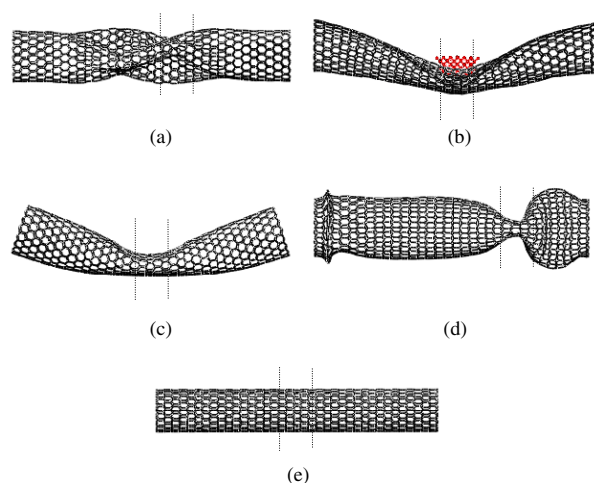


**Figure 1.** The deformed nanotubes having high strain energies under (a) torsion, (b) centre loading, (c) pure bending, (d) compression and (e) tension; the section of the deformed tube used in QM calculations is shown by the dashed lines.

**Table 1.** Binding energies of a hydrogen atom with a nanotube having strain energy of  $2 \text{ kJ mol}^{-1}$ , under various loading conditions.

Deformation	Strain energy ( $\text{kJ mol}^{-1}$ )	$R_{\text{C-H}}$ (Å)	Binding energy ( $\text{kJ mol}^{-1}$ )	Relative binding energy ( $\text{kJ mol}^{-1}$ )
Free tube	0	1.181	193.1	0
Torsion	1.97	1.178	229.9	+36.8
Centre loading	1.95	1.149 (ridge)	314.0	+120.9
Pure bending	1.88	1.174 (ridge)	232.0	+38.9
Compression	2.01	1.183	269.5	+76.4
Tension	2.22	1.178	245.9	+52.8

**Table 2.** Binding energies of a hydrogen atom with a nanotube having high strain energies under various loading conditions.

Deformation	Strain energy ( $\text{kJ mol}^{-1}$ )	$R_{\text{C-H}}$ (Å)	Binding energy ( $\text{kJ mol}^{-1}$ )	Relative binding energy ( $\text{kJ mol}^{-1}$ )
Free tube	0	1.181	193.1	0
Torsion	8.51	1.132 (ridge)	427.1	+234.0
Centre loading	13.93	1.126 (ridge)	321.6	+128.5
		1.188 (flat)	153.1	−40.0
Pure bending	2.95	1.138 (ridge)	398.9	+205.8
Compression	23.06	1.114 (ridge)	480.4	+287.3
Tension	15.71	1.168	236.1	+43.0
	37.21	1.163	258.5	+65.4

### 3.1. Free nanotube

On optimizing the geometry, the hydrogen radical bound to one of the C atoms of the nanotube section, with a C–H bond length of  $1.181$  Å and a binding energy of  $193.1 \text{ kJ mol}^{-1}$ . The C–H bond length and the binding energy with a graphite sheet were  $1.204$  Å and  $110.7 \text{ kJ mol}^{-1}$ , respectively. The higher binding energy with the nanotube C atom could be attributed to the  $\text{sp}^3$  character of the C atoms on rolling a graphite sheet to form the tube. This means that the C atoms of the narrow tube

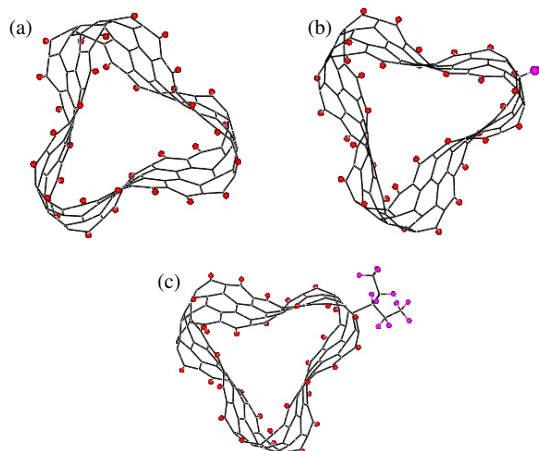


**Figure 2.** (a) Section of the NT under  $40^\circ$  torsional deformation with the hydrogens at the dangling bonds of the perimeter C atoms optimized at DFT/3-21G level, (b) optimized structure of the hydrogen radical at the ridge, and (c) optimized structure of the  $C_5H_{11}$  radical at the ridge.

will have more  $sp^3$  character and hence the deformation energy required to make the C atom tetrahedral is less. Gulseren *et al* [20] found that the binding energy of an adatom decreases with increasing radius of the tube, and eventually saturates at a value corresponding to that of graphite. Our previous quantum mechanics work [7] with alkyl radicals also confirmed that the binding energy decreases as the tube radius increases.

### 3.2. Nanotube under torsion

Under this deformation, the strain energy varied initially cubically with the twisting angle. At the onset of buckling the energy dropped a little and then changed almost linearly. The buckling started at the strain energy of  $7.28 \text{ kJ mol}^{-1}$ , before which the tube retained its cylindrical shape. Sections of the deformed CNT under the strain energy of 1.97 (before buckling) and  $8.51 \text{ kJ mol}^{-1}$  (soon after buckling) were used in the quantum mechanics study. Figure 2(a) shows a section of the tube after buckling, having clear ridges formed on twisting, with H atoms added and optimized to the dangling bonds of the perimeter C atoms. On placing a hydrogen atom near to those tube sections and optimizing its geometry, the hydrogen atom tightly bound to one of the carbon atoms at a ridge with binding energies  $229.9$  (before buckling) and  $427.1 \text{ kJ mol}^{-1}$  (after buckling) respectively. The optimized geometry of the hydrogen bound nanotube section after buckling is shown in figure 2(b). The shorter bond lengths and higher binding energies compared to the hydrogen radical attached to the non-deformed tube (see table 1) show that the deformation promotes the reactivity. This could be explained by the change in hybridization of C atoms. On twisting the nanotube some of the  $sp^2$  hybridized carbon atoms become  $sp^3$  and hence one of the  $sp^3$  hybridized orbitals is free to form a covalent bond with an incoming atom or molecule. On a non-deformed tube the C atoms have only a slight  $sp^3$  character due to the cylindrical shape of the tube, which gives rise to a weak bond with a low binding energy.

On placing an alkyl radical ( $C_2H_5-CH-C_2H_5$ ) near to one of the C atoms at the ridges of the nanotube section of

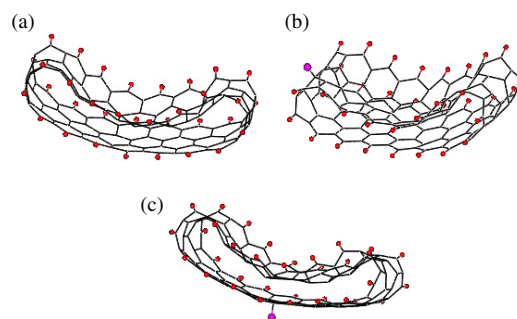


**Figure 3.** (a) Section of the NT under central loading deformation with the hydrogens at the dangling bonds of the perimeter C atoms optimized at DFT/3-21G level, (b) optimized structure of the hydrogen radical at the ridge, and (c) optimized structure of the hydrogen radical at the flattened surface.

figure 2(a), and optimizing its geometry, the radical bound to the C atom, as shown in figure 2(c), with a binding energy of  $337.6 \text{ kJ mol}^{-1}$ . On the other hand, the binding energy between the alkyl radical and a deformation free nanotube is only  $4.3 \text{ kJ mol}^{-1}$  with CNT-alkyl C-C bond length of  $3.7 \text{ \AA}$ . i.e., the alkyl radical does not bind to the free nanotube. It is to be noted that in this calculation only the geometry of the alkyl radical was optimized, like other calculations with deformed tubes, but in our previous work [7] the geometries of both the alkyl radical and the nanotube section were optimized, which gave a binding energy of  $30.5 \text{ kJ mol}^{-1}$ .

### 3.3. Nanotube under centre loading

In this case, the load was applied at the centre of the tube using a spherical indenter while the two ends of the tube were rigidly clamped. The tube started flattening under the indenter at a very early stage. A section of the nanotube with localized deformation was used for the quantum mechanics study. Figure 3 shows clearly that the hydrogen atom bound to one of the C atoms at the ridge. The binding energy was found to be  $314.0 \text{ kJ mol}^{-1}$  when the deformation of the nanotube was mainly localized under the indenter (strain energy =  $1.95 \text{ kJ mol}^{-1}$ ), and  $321.6 \text{ kJ mol}^{-1}$  when further deformation took place (strain energy =  $13.93 \text{ kJ mol}^{-1}$ ), figure 3(b). The binding is fairly strong in both cases. However, when the deformation is localized, one cannot expect strong binding at other places on the tube. Placing a hydrogen atom near to the flattened surface of figure 3(a) gave a lower binding energy of  $153.1 \text{ kJ mol}^{-1}$  and a longer bond length of  $1.188 \text{ \AA}$  (cf  $193.1 \text{ kJ mol}^{-1}$  and  $1.181 \text{ \AA}$  on a free nanotube surface), as shown in figure 3(c). This means that the reactivity of radicals is high at the ridges and low at the flattened surfaces. Again, the increased  $sp^3$  character of the C atoms at the ridges makes the binding strong, whereas the flattened surface behaves like a graphite sheet and as such the binding is weak.

### 3.4. Nanotube under pure bending

Under pure bending, the tube started kinking after reaching a strain energy of  $1.88 \text{ kJ mol}^{-1}$  [12]. Sections of the tube under a strain energy of  $1.88 \text{ kJ mol}^{-1}$  (just before kinking) and  $2.95 \text{ kJ mol}^{-1}$  (soon after kinking; figure 1(c)) were

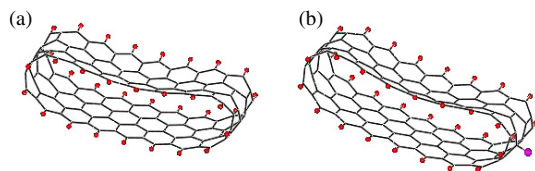


**Figure 4.** (a) Section of the NT under 40° bending deformation with the hydrogens at the dangling bonds of the perimeter C atoms optimized at DFT/3-21G level and (b) optimized structure of the hydrogen radical at the ridge.

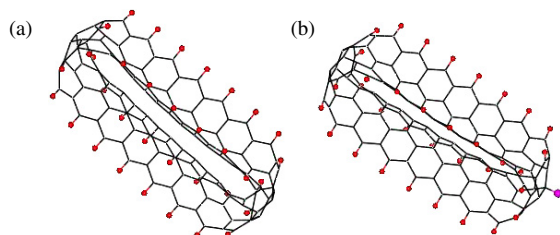


**Figure 5.** (a) Section of the NT under compressive deformation (strain = 0.135) with the hydrogens at the dangling bonds of the perimeter C atoms optimized at DFT/3-21G level and (b) optimized structure of the hydrogen radical at the ridge.

used in the quantum mechanics study. The centre section (kink site) of figure 1(c) with the hydrogen atoms added to the dangling bonds of the perimeter C atoms is shown in figure 4(a). Here again, it has the ridges and flattened portion as in the case with centre loading. The hydrogen atom placed near to the ridge bound to one of the C atoms at the ridge with binding energies of 232.0 kJ mol<sup>-1</sup> (before kinking) and 398.9 kJ mol<sup>-1</sup> (after kinking; figure 4(b)). Although due to ovalization the curvature of the tube changes before kinking, it did not form a well developed ridge and flat surface. Thus the binding energy of radicals was low before kinking.

### 3.5. Nanotube under compression

The tube started buckling once it reached the strain energy of 21.82 kJ mol<sup>-1</sup>. After this, the strain energy started to decrease and increase as it formed more buckles. Sections of the tube having strain energies of 2.01 kJ mol<sup>-1</sup> (before buckling) and 23.06 kJ mol<sup>-1</sup> (soon after buckling; figure 1(d)) were used in the quantum mechanics study. The section of the compressed tube (figure 1(d)) with the hydrogen atoms added to the dangling bonds of the perimeter C atoms is shown in figure 5(a). This section is marked by the dashed lines in figure 1(d). Although it appears like a neck in figure 1(d), it is not narrowed at this point; in fact, this section is almost 90° to the wider section next to it. It is interesting to note that, similar to the sections under centre loading and pure bending with ridges and flattened surfaces, the hydrogen atom placed near the ridge of these sections binds to one of the C atoms with binding energies of 269.5 kJ mol<sup>-1</sup> (before buckling) and 480.4 kJ mol<sup>-1</sup> (after buckling; figure 5(b)). Before buckling, the curvature of the tube did not change significantly when the strain energy was 2.01 kJ mol<sup>-1</sup>, and the binding energy was low.

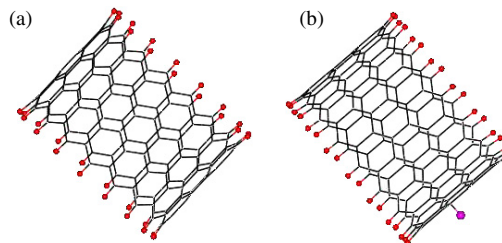


**Figure 6.** (a) Section of the NT under tensile deformation and (b) optimized structure of the hydrogen radical on the deformed section of the NT.

### 3.6. Nanotube under tension

Under this type of loading, the nanotube was stretched along the loading direction and then necked; the necking propagated over the entire length of the tube and formed one atom chain before breaking into two pieces. Sections of tubes having low strain energy of 2.22 kJ mol<sup>-1</sup> and high strain energies of 15.71 and 37.21 kJ mol<sup>-1</sup> (figure 6(a)) are used in the quantum mechanics study. It is to be noted that tensile loading does not generate ridges and flat surfaces like other loadings considered in this work. The hydrogen atom binding energy with the low strain energy section is 245.9 kJ mol<sup>-1</sup> and with the high strain energy section is 258.5 kJ mol<sup>-1</sup>.

In summary, under all types of loading (except tension) the nanotube buckles and forms ridges and flattened surfaces on the tube. Buckling starts at different strain energies for different types of deformation. Of all the deformations studied in this work, under pure bending the tube buckles at rather low strain energy. Quantum mechanics calculations showed that the radicals strongly bind to the C atoms at the ridges; flattened surfaces show even lower binding strength compared to the free tube as they behave like graphite sheet. Comparison of the H atom binding energy under various loading conditions showed that when the strain energy is ~2 kJ mol<sup>-1</sup> (before buckling) centre loading is the best loading method to promote the reactivity. After buckling, pure bending appears to be the best method as it gives a high binding energy when the strain energy is only 2.95 kJ mol<sup>-1</sup>. Under torsion, the ridges are formed along the entire length of the tube and this gives a higher binding energy under relatively low strain energy. Thus this appears to be the best deformation mode to promote multiple reactions on nanotubes. Srivastava *et al* [21] also predicted that the chemisorption of hydrogen atoms is enhanced by ~1.6 eV (i.e. ~154.4 kJ mol<sup>-1</sup>) at regions of high deformation due to bending and torsion of SWNTs. Park *et al* [22] developed a model to predict the chemical reactivity of CNTs quantitatively from their initial structures and found that the hydrogenation energy is enhanced at the kink site of bent CNTs—further confirming the above results. Among the axial loadings of compression and tension, compression provides a much higher binding energy at relatively high strain energy of 23.1 kJ mol<sup>-1</sup>. Even under high strain energy of 37.21 kJ mol<sup>-1</sup>, tension deformation does not increase the reactivity of hydrogen radical considerably.

Finally it is interesting to note that the reaction on nanotubes changes the bandgap, which is calculated as the

difference in energy between the highest occupied molecular orbital (HOMO) and the lowest unoccupied molecular orbital (LUMO). A significant increase in bandgap is observed on binding a hydrogen atom to the nanotube. This means the adsorption of the hydrogen atom on the nanotube will lead to a decrease in conductance. This is because the change in bonding configuration from  $sp^2$  to  $sp^3$  on the adsorption of hydrogen atom is accompanied by a decrease in  $\pi$ -electron density, that is responsible for electrical conductance. Thus the chemical reaction on the nanotube surface modifies the electronic structure, that could lead to the fabrication of novel nanoscale devices.

It is worth mentioning that in the blending of CNT-polymer composites a CNT is often under a combined loading, including many of the loading modes studied above. Furthermore, because of the large aspect ratio of CNTs, multiple kinking/buckling (maybe hundreds) may form on a single CNT. These, according to our discussion above, will enhance the formation of chemical bonds.

#### 4. Conclusion

Our study reveals important and novel information on the reactivity of mechanically deformed CNTs. All deformation modes promote reactivity with H atoms. The CNTs deformed by centre loading and compression bind atoms and radicals strongly at the ridges when the strain energy is as low as  $\sim 2$  kJ mol<sup>-1</sup>. Pure bending shows a much stronger binding when the strain energy is little higher than 2 kJ mol<sup>-1</sup>. A CNT under torsion also shows strong binding, albeit at higher strain energy and higher applied force than pure bending. Thus mechanical deformations in composite blending can promote reactivity with nearby chemical species without adding specific chemical reagents to functionalize the nanotubes.

#### Acknowledgments

The authors thank the Australian Research Council for its continuous financial support. This work was also supported by the Australian Partnership for Advanced Computing.

#### References

- [1] Zhou C, Kong J, Yenilmez E and Dai H 2000 *Science* **290** 1552
- [2] Kong J, Franklin N R, Zhou C, Chapline M G, Peng S, Cho K and Dai H 2000 *Science* **287** 622
- [3] Xiao K Q and Zhang L C 2004 *J. Mater. Sci.* **39** 4481
- [4] Bauschlicher C W 2000 *Chem. Phys. Lett.* **322** 237
- [5] Bauschlicher C W 2001 *Nano Lett.* **1** 223
- [6] Jaffe R L 2003 *J. Phys. Chem. B* **107** 10378
- [7] Mylvaganam K and Zhang L C 2004 *J. Phys. Chem. B* **108** 5217
- [8] Mylvaganam K and Zhang L C 2004 *J. Phys. Chem. B* **108** 15009
- [9] Brenner D W 1990 *Phys. Rev. B* **42** 9458
- [10] Brenner D W, Shenderova O A, Harrison J, Stuart S J, Ni B and Sinnott S B 2002 *J. Phys.: Condens. Matter* **14** 783
- [11] Mylvaganam K and Zhang L C 2004 *Carbon* **42** 2025
- [12] Mylvaganam K and Zhang L C 2005 *J. Comput. Theor. Nanosci.* **2** 251
- [13] Becke A D 1988 *Phys. Rev. A* **38** 3098
- [14] Lee C, Yang W and Parr R G 1988 *Phys. Rev. B* **37** 785
- [15] Vosko S H, Wilk L and Nusair M 1980 *Can. J. Phys.* **58** 1200
- [16] Becke A D 1993 *J. Chem. Phys.* **98** 5648
- [17] Binkley J S, Pople J A and Hehre W J 1980 *J. Am. Chem. Soc.* **102** 939
- [18] D'Souza F, Zandler M E, Smith P M, Deviprasad G R, Arkady K, Fujitsuka M and Ito O 2002 *J. Phys. Chem. A* **106** 649
- [19] Frisch M J *et al* 2004 *Gaussian 03* (Wallingford CT: Gaussian, Inc.)
- [20] Gulseren O, Yildirim T and Ciraci S 2001 *Phys. Rev. Lett.* **87** 116802
- [21] Srivastava D, Brenner D W, Schall J D, Ausman K D, Yu M and Ruoff R S 1999 *J. Phys. Chem. B* **103** 4330
- [22] Park S, Srivastava D and Cho K 2003 *Nano Lett.* **3** 1273